Journal of Korea Multimedia Society Vol. 24, No. 5, May 2021(pp. 642-650)
https://doi.org/10.9717/kmms.2021.24.5.642

An Automatic Strabismus Screening Method with Corneal Light Reflex based on Image Processing

Xi-Lang Huang[†], Chang Zoo Kim[††], Seon Han Choi[†††]

ABSTRACT

Strabismus is one of the most common disease that might be associated with vision impairment. Especially in infants and children, it is critical to detect strabismus at an early age because uncorrected strabismus may go on to develop amblyopia. To this end, ophthalmologists usually perform the Hirschberg test, which observes corneal light reflex (CLR) to determine the presence and type of strabismus. However, this test is usually done manually in a hospital, which might be difficult for patients who live in a remote area with poor medical access. To address this issue, we propose an automatic strabismus screening method that calculates the CLR ratio to determine the presence of strabismus based on image processing. In particular, the method first employs a pre-trained face detection model and a 68 facial landmarks detector to extract the eye region image. The data points located in the limbus are then collected, and the least square method is applied to obtain the center coordinates of the iris. Finally, the coordinate of the reflective light point center within the iris is extracted and used to calculate the CLR ratio with the coordinate of iris edges. Experimental results with several images demonstrate that the proposed method can be a promising solution to provide strabismus screening for patients who cannot visit hospitals.

Key words: Automatic strabismus screening, Corneal light reflex, Image processing

1. INTRODUCTION

Vision plays an important role for people to understand and interact with the environment. Normal vision can ensure the accurate cognition of things and give us depth perception. However, many ocular diseases often occur and affect our daily life. Among all the ocular diseases, strabismus is one of the most common eye conditions, which affects 5.4% of the population of the USA and commonly occurs in children[1]. Strabismus is a condition in which the eyes do not align with each other when focusing on an object. Many factors may cause strabismus, such as muscle dysfunction, farsightedness, and problems on the optic nerve, etc. According to the eyes' position, strabismus can be divided into 4 types. When one eye or both eyes turn either inward, it is known as esotropia, and the opposite condition is called exotropia, in which one or both eyes turn outward. When one eye turns upward, it is called hypertropia, and hypotropia indicates that one eye turns downward. Due to the misalignment of the eyes, strabismus can lead to vision impairment and faulty depth perception. If the strabismus is not diagnosed and corrected, it may go on develop to am-

※ Corresponding Author : Seon Han Choi, Address: (48513) 45 Yongso-ro, Nam-gu, Busan, Korea, TEL : +82-51-629-6240, FAX : +82-51-629-6230, E-mail : shchoi@pknu.ac.kr
Receipt date : Apr. 26, 2021, Revision date : May 17, 2021
Approval date : May 20, 2021

[†] Dept. of Artificial Intelligent Convergence, Pukyong National University (E-mail : huangxl901@pukyong.ac.kr)
[††] Dept. of Ophthalmology, Kosin University College of Medicine (E-mail : changzoo@hanmail.net)
[†††] Dept. of IT Convergence and Application Engineering, Pukyong National University
※ This work was supported by a Research Grant of Pukyong National University(2021)

blyopia, which leads to permanently decreased vision.

So far, there are a variety of tests that can screen strabismus for clinical diagnostic purposes, such as the prism cover test (PCT), the red reflex test (RRT), and the Hirschberg test (HT). The PCT (also known as the golden standard) places an occlude over one eye and uses a prism bar to measure the deviation of the uncovered eye for strabismus screening. Despite this test can provide a reliable measurement of ocular misalignment, it can only be performed manually by a well-trained ophthalmologist. The RRT is performed by projecting the ophthalmoscope light onto the patient's eyes from approximately 18 inches away in a darkened room[2]. Different from the PCT, the RRT has the advantage of being simple, fast, and requires less labor[3]; however, it is limited to be performed under certain conditions. The HT, so- called corneal light reflex (CLR) test, is another strabismus screening test in which an ophthalmologist shines light into the eyes of a patient to see if the light in the two eyes is symmetrical. Although HT is the quickest and simplest way to measure ocular alignment among these tests, it still requires manual operation and can only be performed in hospitals, which is infeasible for people with poor medical access.

To help screen strabismus for the people who cannot visit the hospitals or eye care centers, this work proposed an automatic strabismus screening method with CLR based on image processing. The proposed method includes 5 steps to obtain the screening result. (1) Face detection with a pre-trained face detection model; (2) Facial landmark model for eye region detection; (3) Binarization with Otsu's binarization and HSV color model; (4) Localization of limbus with the least square method (LSM); and (5) CLR ratio estimation based on the limbus and reflective points.

The rest of this study is organized as follows: Section II provides the background of the image processing methods for the study, and Section III describes the proposed method. Section IV shows the experimental results, and a brief conclusion is given in Section V.

2. BACKGROUND

In this section, we briefly introduce the image processing techniques used in the proposed method. They are the face detection model, facial landmark detector, Otsu's binarization, and HSV color space.

2.1 Face detection model

In this study, the proposed method firstly used a face detection model to extract facial parts from a digital image, which is also the foundation for successful strabismus screening. However, the successful detection of faces in images usually affected by many factors such as illumination, resolution, and occlusion within the image. Therefore, an accurate and stable face detection model that can handle various situations is essential in this study. With the rapid development of deep learning, the use of deep learning methods, namely the convolutional neural network (CNN), for face detection has achieved a lot of successful progress and shown remarkable performance in various scenes, which could be attributed to its enormous learning capacity and learnable feature extractors. To perform accurate and reliable face detection for the images taken under various scenes, our method employs a CNN-based face detection model provided by the dlib library. The model is obtained by training a CNN on the images from ImageNet, PASCAL VOC, VGG with the use of maximum margin object detection algorithm [4] as the loss function.

2.2 Facial landmark detector

If the face within the image can be detected, a facial landmark detector will be employed to extract the region of interest (ROI). Dlib library pro-

vides a 68 facial landmark detector that is made using the ensemble of regression trees[5], and pre-trained on the IBUG 300-W dataset[6], which aims to help the detector extract the 68 facial landmarks from the labeled face images taken under different situations. The extracted facial landmarks by the detector are shown in Fig. 1. All the landmarks are represented by the index array from 1 to 68. To extract the eye region from the detected face image, our method utilizes the index of 37 and 46 to create a square region that two eyes are included.

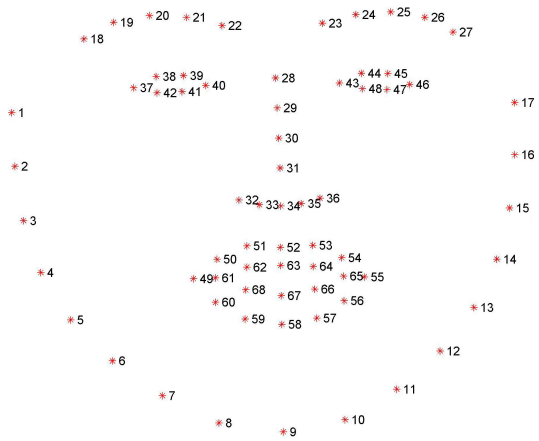

Fig. 1. A pre-trained 68 facial landmark detector.

2.3 Otsu's binarization

In image processing, binarization is usually used to keep the ROI in the images while neglecting the backgrounds that we are not concerned with. To achieve this, an optimal threshold value that enables separate the target object from the irrelevant object should be pre-defined, which is totally depends on the experience of the designer. However, each designer has a different perception of an image, and the brightness of each image is different, manually selecting the optimal threshold value for various images to locate the objective is tedious and infeasible. Considering this issue, our method employs Otsu's binarization[7], which can automatically determine the optimal threshold rather than selecting a fixed threshold value. This binarization method determines the optimal threshold value that minimizes intra-class intensity variance by enumerating all the possible greyscale levels generated by the histogram. In this study, Otsu's binarization was used to eliminate the influences of the skin color and the sclera (i.e., the white of the eye) to the iris localization.

2.4 HSV color model

Although the binarization method mentioned above could eliminate a big part of irrelevant objects from the eye region image. However, it may fail at distinguishing the object that has a similar color space with the iris, such as the shadows in the internal and medial canthus, shadows between the sclera and the lower eyelid, and the eyelash. To deal with this problem, the HSV color model is used to extract the desired object with a pre-defined color space value. The HSV color model is an alternative representation of the RGB color model, where H, S, V represent hue, saturation, and value respectively. Owing to its capability of separating the brightness from the chromaticity, it has been widely used in image classification[8-10], and image segmentation[11-13] as it can detect a target object with a certain color. The HSV color model in this work is used as a supplement binarization method that focuses on extracting the iris region.

3. METHOD

3.1 Overview of the proposed method

The screening of strabismus in digital images depends on the precise location of reflective points and the limbus. Therefore, the proposed method was organized into 5 steps to complete the procedure of strabismus screening, which is shown in Fig. 2. The input is a digital image that has a resolution of 1920x1280. The image first goes through the face detection model and the facial landmark detector to obtain the eye region landmarks, and

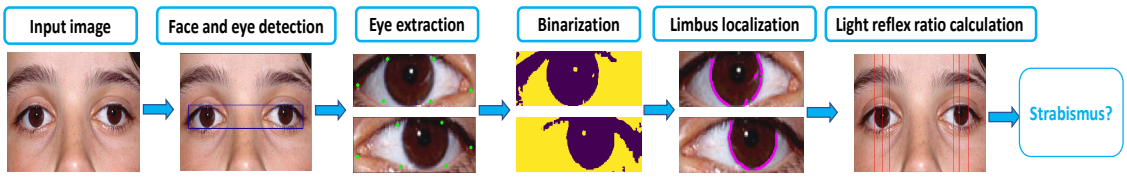

Fig. 2. Overview of the proposed method.

then the left and right eye are extracted based on its landmarks. Binarization is applied to the extracted eye images to eliminate the influence factors while maintaining the iris region. With the processed images, the method calculates the center coordinates of the reflective points and samples the data points that lie in the limbus to estimate the center of the iris, which can be used to obtain the coordinates of the limbus. Finally, the CLR ratio for strabismus screening is calculated according to the coordinates of the limbus and the reflective point center.

3.2 Face and eye detection

At the preliminary stage of the proposed method, a facial image was sent to the face detection model. To reduce the memory occupation for face detection, the image was resized to its half size, namely 860×640. If a face can be detected within the image, the model returns the coordinate of a rectangular bounding box that enclosed the facial part within the image. With the coordinates of the detected facial part, the facial landmark detector is applied to estimate the location of 68 coordinates that match the facial structures on the detected face. For positioning the eye, we only utilize the indexes from 37 to 48 in this study.

3.2 Eye extraction

As shown in Fig. 1, the index array for the right eye region is from 37 to 42, and 43 to 48 for the left eye region. To extract the eye region from the image, we utilize the coordinates of these landmarks. For the extraction of the right eye region, the width value of the index 37 and the height value of the index 38 are used as the beginning coordinate, the width value of the index 40 and the height value of 41 are used as the ending coordinate. With the similar operation above, the left eye region can also be extracted. However, the detector may not accurately locate the facial landmarks for the eye region, which affects the extraction of the complete eye region. To tackle this problem, we add a parameter that enlarges the size of the extracted eye region image. In other words, the parameter simultaneously increase the height and width of the image to ensure a complete eye region can be included, which is shown in the eye extraction block in Fig. 2.

3.2 Binarization

If the eye regions are obtained, the method implements Otsu's binarization and HSV color model to remove the objects that affect the acquisition of the iris center. First, the eye region images are filtered with a 5×5 Gaussian kernel to remove the noises that exist in the image. Then, the next step is to convert the eye region image into grayscale and apply binary thresholding to remove the skin and sclera (the white part around the iris), so that only the iris region remains. However, since the images have different illumination, a fixed threshold value cannot meet the requirement of iris extraction. Thus, we utilize Otsu's binarization to automatically determine the threshold value. With the optimal threshold value determined by Otsu's binarization, the pixel values smaller than the determined threshold value are set to 0 (black) and the pixel values bigger than the threshold value are set to 255 (white). Despite Otsu's binarization can

remove most of the background of the eye region, but some black backgrounds (i,e., the shadow generated by the eyelid) are remained and affect the result of iris extraction. Due to the pixels of the shadow is easily affected by the illumination, its pixels' value is bigger than the value of the iris. Thus, the proposed method further converts the eye region image from the RGB color model to the HSV color model by setting the array of the upper bound color and lower bound color, which is consists of the value of 3 channels. The arrays aim to keep the object if the pixel value of the object falls within the pre-defined upper and lower bound, otherwise remove. The HSV-type image may contain less shadow than the binarization image, but it may be susceptible to the pre-defined color value. From this point of view, the direct use of the HSV-type image may cause pixel loss inside the iris. Therefore, we combine the binarization image and HSV-type image to form a new image with fewer shadows while maintaining the iris region, which is shown in Fig. 3.

3.4 Limbus localization

The limbus is the boundary of the cornea and the sclera. To determine the right and left edges from the limbus coordinates, our method utilizes the center coordinate and radius of the iris that can be obtained by the LSM. Firstly, since the iris usually locates at the center of the extracted eye region image, we assume the coordinate of this center is within the iris region. If the pixel value of the coordinate is 0, which indicates that the assumed point is not within the iris region. Then, we use the height value of the assumed point to search for the iris region along the width of the image until the width value has the pixel value of 255. Secondly, the method uses the coordinate obtained in the first step to searches for the maximum height value (bottom) of the iris region by comparing the coordinate whose pixel value is 255. It is noted that the coordinates that lie on the limbus are the last coordinates with the pixel value of 255. Using this property, the method can sample the coordinates located at the limbus from the coordinates obtained in the second step. Fig 4 visualizes the result of the sampled coordinates.

To determine the right and left edge of the iris for both eyes, one simple idea is to compare all the width values of the sampled coordinates. However, the coordinates sampled from the limbus may not be perfectly accurate, which affects the determination of the right and left edges of the iris. Thus, we employed the LSM to approximate the coordinates with a circle, which aims to estimate the center of the iris by minimizing the mean square geometric distance from the circle to the coor-

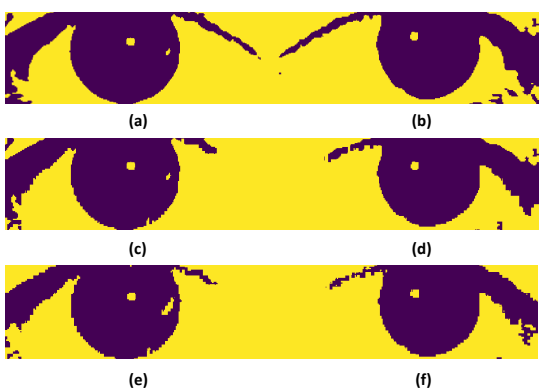

Fig. 3. Image processing for the eye region image, where (a) and (b) are the result of Otsu's binarization, (c) and (d) are the results of the HSV color model, and (e) and (f) are the results of the combination of two methods.

Fig. 4. Visualizing the sampled coordinates on the limbus, where the pink dots are the coordinate points.

dinates. We define the above problem following [14]:

$$\min \sum_{i=1}^{n} \left(\sqrt{(x_i - a)^2 + (y_i - b)^2} - R \right)^2 \quad (1)$$

where n is the total number of coordinates, (x_i, y_i) is the coordinate of the ith coordinate, (a,b) is the center of the circle, and R is its radius. Since (a,b) is not known in advance, it is set as the mean of the coordinates. Fig. 5 shows the result of iris center estimation.

Having the coordinates of the iris center, the left and right edges of the irises of the two eyes can be determined. That is, the edges of the iris can be calculated by adding or subtracting the radius of the circle from the coordinates of the iris center.

3.5 Corneal light reflex ratio calculation

In the final stage of the method, the coordinate of the reflective light points is estimated and used to calculate the CLR ratio. To obtain the coordinates from the image, we extract the iris region image based on the coordinate of the iris center and convert it to grayscale. The next step is to apply Otsu's binarization method to the grayscale and store all the coordinates of the reflective light points. Using these coordinates, we can obtain the center coordinate of the reflective light points by calculating their average value. After the coordinates of the iris edges and the reflective light point center are obtained, we use them to calculate 2 horizontal distances for each eye, which is shown in Fig. 6.

To compute the CLR ratio for strabismus screening, we follow the formula from [15]:

$$Corneal\ light\ reflex\ ratio = \frac{D_1 + D_3}{D_2 + D_4} \quad (2)$$

With the computed value, the method takes it to compare with the reference table of CLR ratio, as shown in Table 1, to determine whether the patient is suffering from strabismus. If the computed value falls within the normal range, it means that the patient's eyes are normal; otherwise, if the value falls within the abnormal range, it is considered that the patient has strabismus.

4. EXPERIMENTAL RESULTS

In this study, 20 images (10 normal eyes, 10 strabismus) were used to test the proposed method. The images were provided from Kosin University Gospel Hospital and labeled by an ophthalmologist. All the images have a resolution of 1920x1280. The method was implemented with an eight-core AMD Ryzen 7 2700 CPU and was based on python

Fig. 5. Visualizing the estimated iris center, where the red dots represent the iris center.

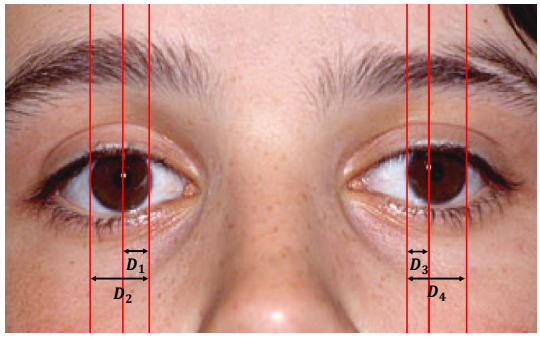

Fig. 6. Horizontal distance measurements from the image.

Table 1. Normal and abnormal ranges of CLR ratio[15].

Parameter	Measurement
Normal range	0.448-0.488
Abnormal range	<0.440, >0.497

(version 3.7.9) and OpenCV (version 3.4.2). We set the parameter that enlarges the size of the extracted eye region as 10, which means that the height and width of the eye region extracted from the landmarks will be simultaneously increased by 10-pixel units. For the HSV color model, we set the upper bound color as [180, 255, 49] and the lower bound color as [0, 0, 0], which aim to remove the shadows. The result of the measured CLR ratio of the images is shown in Table 2.

From Table 2, we can see that the CLR ratio of the normal image falls within the range of 448 to 488, while the ratio of the strabismus image falls within the range of <0.440 and > 0.497, indicating the effectiveness of the proposed method. In addition, we observe that the estimated distances D_2 and D_4 have very similar values, and the error between them may likely be caused by the approximation of the sampling points during iris extraction.

In the measurements of the Normal images, the difference between D_1 and D_3 is caused by the localization of the reflective point center. For example, D_2 and D_4 on the image of ID 6 have almost equal estimates and D_1 and D_3 are also supposed to be similar. However, since the center of the reflection point is estimated from the average of all reflected points, the approximation error for each iris will lead to the difference between D_1 and D_3. In the results of strabismus images, since there are two types of strabismus, exotropia (eyes deviate outward) and esotropia (eyes turn inward), the estimated CLR ratio fall within the range of >0.497 and <0.440.

Table 2. Measurement of CLR ratio for 20 images.

ID	Label	D_1	D_2	D_3	D_4	CLR ratio	Screening result
1	Normal	41.309	87.976	43.486	90.267	0.476	Normal
2	Normal	54.172	100.745	42.860	98.898	0.486	Normal
3	Normal	30.242	67.222	29.661	63.542	0.458	Normal
4	Normal	50.065	108.557	53.174	113.636	0.465	Normal
5	Normal	32.968	80.054	38.985	77.769	0.456	Normal
6	Normal	42.946	96.256	48.748	96.922	0.475	Normal
7	Normal	42.863	82.035	35.156	81.851	0.476	Normal
8	Normal	30.546	72.988	34.973	72.426	0.451	Normal
9	Normal	36.167	89.769	44.361	89.509	0.449	Normal
10	Normal	39.063	83.125	38.834	81.882	0.472	Normal
11	Strabismus	21.244	66.488	35.579	68.557	0.421	Abnormal
12	Strabismus	44.114	89.537	78.856	93.199	0.672	Abnormal
13	Strabismus	8.395	58.873	33.344	65.099	0.336	Abnormal
14	Strabismus	14.729	84.487	31.527	89.033	0.267	Abnormal
15	Strabismus	35.926	117.609	25.891	112.719	0.268	Abnormal
16	Strabismus	44.523	117.354	23.194	115.122	0.291	Abnormal
17	Strabismus	32.918	75.346	23.890	72.646	0.384	Abnormal
18	Strabismus	61.719	97.631	38.243	92.066	0.527	Abnormal
19	Strabismus	9.299	57.324	28.700	61.219	0.321	Abnormal
20	Strabismus	17.370	60.874	34.187	62.249	0.419	Abnormal

Despite the success of the proposed method, there are still some limitations are required further improvement. 1) Due to the HSV color model requires pre-defined upper and lower bound color to extract the desired color, it may fail when the iris color is different from the pre-defined color value. 2) The estimate of the reflective point center has a big impact on the measurement of CLR ratio. From this point of view, a much more stable and accurate binarization method is required to locate the reflective point center.

5. CONCLUSIONS

In this study, in order to provide strabismus screening for patients who cannot visit hospitals in remote areas, we propose an automatic strabismus screening method that compares CLR on both eyes in a facial image. The method employed a face detection model, facial landmark detector, automatic binarization, and the least square method to locate the coordinates of the iris edges and the reflective point center. These estimated coordinates are used to compute CLR ratio for determining whether a patient is suffering strabismus. The experimental results with several images demonstrate the effectiveness of the proposed method.

REFERENCE

[1] B.G. Mohney, “Common forms of childhood esotropia,” *Ophthalmology*, Vol. 108, No. 4, pp. 805-809, 2001.

[2] S.P. Donahue, C.N. Baker, and Committee on

Practice and Ambulatory Medicine, "Procedures for the Evaluation of the Visual System by Pediatricians," *Pediatrics*, Vol. 137, No. 1, pp. 2015-3597, 2016.

[3] A.C. Tongue and G.W. Cibis, "Bruckner test," *Ophthalmology*, Vol, 88, No. 10, pp. 1041-1044, 1981.

[4] D.E. King, "Max-Margin Object Detection," arXiv:1502.00046, 2015.

[5] V. Kazemi and J. Sullivan, "One Millisecond Face Alignment with an Ensemble of Regression Trees," *Proceedings of IEEE Conference on Computer Vision and Pattern Recognition,* pp. 1867-1874, 2014.

[6] C. Sagonasa, E. Antonakosa, G. Tzimiropoulosb, S. Zafeirioua, and M. Pantic, "300 Faces In-The-Wild Challenge: database and results," *Image and Vision Computing,* Vol. 47, pp. 3-18, 2016.

[7] N. Otsu, "A Threshold Selection Method from Gray-level Histograms," *IEEE Transactions on Systems, Man, and Cybernetics*, Vol. 9, No. 1, pp. 62 - 66, 1979.

[8] O.R. Indriani, E.J. Kusuma, C.A. Sari, E.H. Rachmawanto, and D.R.I.M. Setiadi, "Tomatoes Classification using K-NN based on GLCM and HSV Color Space," *Proceedings of International Conference on Innovative and Creative Information Technology*, pp. 1-6, 2017.

[9] H. Razalli, R. Ramli, and M.H. Alkawaz, "Emergency Vehicle Recognition and Classification Method Using HSV Color Segmentation," *Proceedings of IEEE International Colloquium on Signal Processing & Its Applications*, pp. 284-289, 2020.

[10] Y.A. Gerhana, W.B. Zulfikar, A.H. Ramdani and M.A. Ramdhani, "Implementation of Nearest Neighbor using HSV to Identify Skin Disease," P*roceedings of the 2nd Annual Applied Science and Engineering Conference*, pp. 1-5, 2017.

[11] S. Sural, G. Qian, and S. Pramanik, "Segmentation and Histogram Generation using the HSV Color Space for Image Retrieval," *Proceedings of IEEE International Conference on Image Processing*, pp. 589-592, 2002.

[12] E. Prasetyo, R.D. Adityo, N. Suciati and C. Fatichah, "Mango Leaf Image Segmentation on HSV and YCbCr Color Spaces using Otsu Thresholding," P*roceedings of International Conference on Science and Technology-Computer*, pp. 99 - 103, 2017.

[13] N.R. Choi and S.I. Choi, "Preprocessing Technique for Lane Detection Using Image Clustering and HSV Color Model," *Journal of Korea Multimedia Society*, Vol. 20, No. 2, pp. 144-152, 2017.

[14] N. Chernov and C. Lesort, "Least Squares Fitting of Circles and Lines," *Computer Vision and Pattern Recognition*, 2003.

[15] S. Duangsang and S. Tengtrisorn, "The Central Corneal Light Reflex Ratio from Photographs derived from a Digital Camera in Young Adults," *Journal of the Medical Association of Thailand*, Vol. 95 No. 5, pp. 699-703, 2012.

Xi-Lang Huang

He received the M.S. degree in electrical engineering from the Pusan National University, Busan, South Korea, in 2018. He is currently pursuing the Ph.D. degree in electrical engineering with the Pukyong National University, Busan, South Korea. His current research interests include modeling and simulation of discrete-event systems, efficient simulation optimization, and computer vision.

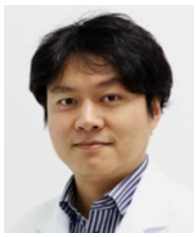

Chang Zoo Kim

He received the M.D. and M.S. degrees from the Kosin University College of Medicine, Busan, South Korea, in 2011 and 2019, respectively. In 2017. he become an Ophthalmologist, and specialized in Strabismus and Pediatric Ophthalmology in 2018. In 2019, he joined the Department of Ophthalmology, Kosin University College of Medicine, as an Assistant Professor. His current research interests include medical devices based on artificial intelligence and strabismus.

Seon Han Choi

He received the B.S., M.S., and Ph.D. degrees in electrical engineering from the Korea Advanced Institute of Science and Technology (KAIST), Daejeon, South Korea, in 2012, 2014, and 2018, respectively. He was a Teaching Assistant for computer programming with the School of Electrical Engineering, from 2013 to 2017. In 2018, he was a Post-Doctoral Researcher with the Information and Electronics Research Institute, KAIST. From 2018 to 2019, he was a Senior Researcher with the Korea Institute of Industrial Technology. In 2019, he joined the Department of IT Convergence and Application Engineering, Pukyong National University, Busan, South Korea, as an Assistant Professor. His current research interests include the modeling and simulation of discrete-event systems, efficient simulation optimization under stochastic noise, evolutionary computing, and machine learning.